Coexistence of Excitability, Hopf and Turing Modes in a One-Dimensional Array of Nonlinear Circuits

Moncho Gómez-Gesteira, Vicente Pérez-Muñuzuri, Leon O. Chua, *Fellow, IEEE*, and Vicente Pérez-Villar

***Abstract*—The behavior in the vicinity of a point where excitable, Hopf and Turing modes coexisting is analyzed within the framework of a simplified version of Chua's nonlinear circuits. The different factors (e.g., initial and boundary conditions and small changes in circuit parameters) which determine the final state of the system are numerically studied.**

I. Introduction

In his classic 1952 paper [1], Turing suggested the possibility of spontaneous formation of stationary patterns in a system where only reaction and diffusion (RD) were involved. Nevertheless, it was necessary to wait until 1990 [2], [3] to obtain experimental evidence of such patterns; generally called Turing patterns. From then on, considerable efforts have been devoted both theoretically and experimentally to the characterization of the different patterns and to the study of their relationships with similar structures observed in biological systems [4]. Even recently, much interest has been focused both on the appearance of self-replicant spots [5]–[7] and on the interaction between Turing and Hopf modes [1], [8]–[10].

On the other hand, it is well known that an array of Chua's circuits, which can be described by means of a set of ODE's, can exhibit most of the phenomena typically found in RD systems; namely, spiral waves [11], travelling waves [12], chaotic behavior [13] and Turing patterns [14], [15]. This kind of system has some important advantages when compared to continuous (chemical) systems, because both the excitability of each cell and their diffusion can be externally controlled, which cannot, obviously, be done in chemical or biological systems.

Throughout this paper, we will study the behavior of an array of Chua's circuits in the vicinity of a triple point, where Turing and Hopf modes and a trivial stable state coexist.

Manuscript received January 5, 1995; revised April 24, 1995. This work was supported in part by *Xunta de Galicia* under Project XUGA20611B93. This paper was recommended by Guest Editor L. O. Chua.

M. Gómez–Gesteira, V. Pérez–Muñuzuri, and V. Pérez–Villar are with the Group of Nonlinear Physics, Faculty of Physics, University of Santiago de Compostela, 15706 Santiago de Compostela, Spain.

L. O. Chua is with the Group of Nonlinear Physics, Faculty of Physics, University of Santiago de Compostela, 15706 Santiago de Compostela on leave from the Department of Electrical Engineering and Computer Sciences, University of California, Berkeley, CA 94720 USA.

IEEE Log Number 9414475.

II. Model

As it was previously mentioned, we will use a set of discretely-coupled dynamic systems where each cell is described by a Chua circuit [16], [17]. This system can be described by the set of ODE's

$$\begin{aligned}\dot{u}_i &= \alpha[v_i - h(u_i)] + D_u[u_{i+1} - 2u_i + u_{i-1}]\\ \dot{v}_i &= u_i - v_i + w_i + D_v[v_{i+1} - 2v_i + v_{i-1}]\\ \dot{w}_i &= -\beta v_i - \gamma w_i\end{aligned} \tag{1}$$

where $h(u)$ describes a three-segment piecewise-linear function

$$h(u) = m_1 u + 0.5(m_o - m_1)(|u+1| - |u-1|) + \varepsilon. \tag{2}$$

In order to obtain a simpler system, the set of (1) can be transformed by supposing w changes with a significantly faster time scale so w is determined by the instantaneous values of the other variables according to

$$w = -\frac{\beta}{\gamma} v \tag{3}$$

obtained by setting $\dot{w}_i = 0$ in (2). This approximation is equivalent to replacing the inductor in Chua's circuit by a short circuit, thereby obtaining a second-order *reduced* Chua's circuit.

Thus, the new two-variable system will be described by

$$\begin{aligned}\dot{u}_i &= f(u_i, v_i) + D_u[u_{i+1} - 2u_i + u_{i-1}]\\ \dot{v}_i &= g(u_i, v_i) + D_v[v_{i+1} - 2v_i + v_{i-1}]\end{aligned} \tag{4}$$

with

$$\begin{aligned}f(u_i, v_i) &= \alpha[v_i - h(u_i)]\\ g(u_i, v_i) &= u_i - \nu v_i\end{aligned} \tag{5}$$

where

$$\nu = \frac{\gamma + \beta}{\gamma}.$$

The set of fixed parameters we will use throughout this paper is $\{\alpha, m_o, m_1, D_u, D_v\} = \{-10.0, -1.0, 0.1, 1.0, 40.0\}$. The parameters ν and ε will be considered free parameters, though their values will be restricted to the intervals $\varepsilon \in [0, 4]$ (since the effects due to ε are symmetric for positive and

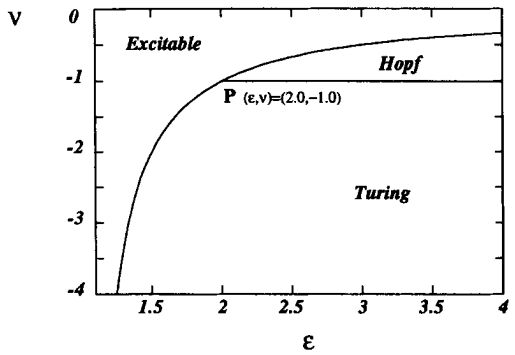

Fig. 1. The (ε, ν) parameter space. For the set of parameters $\{\alpha, m_o, m_l, D_u, D_v\} = \{-10.0, -1.0, 0.1, 1.0, 40.0\}$, three different regions were identified for different (ε, ν) values: excitable, Turing and Hopf. Note the existence of a point $\boldsymbol{P}$ where these three states coexist.

negative values), and $\nu \in [-4.0, -0.1]$, (since only for negative values of ν can Turing structures be obtained and since the system can exhibit three equilibrium points (bistability) if $\nu > -0.1$, and we are only interested in systems with a sole critical point). Moreover, within the above parameter intervals, it is possible to find a point where three different states can coexist.

If we let f_u, f_v, g_u, and g_v denote the partial derivatives of $f(u,v)$ and $g(u,v)$ evaluated at the dc steady state (equilibrium point), we can study the stability of that equilibrium point when only reaction terms[1] are taken into account. So, an equilibrium point is stable if

$$f_u + g_v < 0 \tag{6a}$$

$$f_u g_v - f_v g_u > 0. \tag{6b}$$

On the other hand, when diffusive terms are taken into account, a stable point (satisfying (6a) and (6b)) can give rise to a Turing instability. To obtain this behavior, two new conditions must be imposed

$$f_u D_v + g_v D_u > 0 \tag{7a}$$

$$(f_u D_v + g_v D_u)^2 - 4 D_u D_v (f_u g_v - f_v g_u) > 0. \tag{7b}$$

So, in the (ν, ε) parameter space, three different regions can be considered, namely; (a) *excitable region*, which corresponds to those parameter values fulfilling conditions (6a) and (6b). Physically, this corresponds to the existence of an excitable stable point, which can execute a large excursion in the phase space after being perturbed beyond a certain threshold. This is equivalent to a monostable or single-shot electronic circuit; (b) *Hopf region*, which corresponds to parameter values where at least one of the previous conditions ((6a) or (6b)) is not fulfilled, so there exists an unstable equilibrium point and a stable limit cycle around it; (c) Finally, there is a *Turing region* where (6a), (6b) and (7a), (7b) are fulfilled (the system can be driven unstable by diffusion). The spatially homogeneous state is stable, but it can become unstable due to any small perturbation, and will eventually tend to a stationary but nonhomogeneous structure. In Fig. 1, the three regions are represented as a function of the parameters (ν, ε). Observe the existence of a critical point $P(\nu_t = -1.0, \varepsilon_t = 2.0)$, where the three states coexist.

In the next section, we will study the different conditions that will influence the system behavior when initially placed in the vicinity of the triple point P. Throughout our calculations we will always consider the same computational space (500 circuits) and an explicit Euler method with a time step $\Delta t = 10^{-3}$.

[1] In this paper, we adopt the standard terminology on Turing patterns, where "*reaction terms*" means without diffusion ($D_u = D_v = 0$). In circuit terminology, this is equivalent to investigating a single "*uncoupled*" Chua's circuit.

III. System Evolution Near a Triple Point

A. Influence of Initial Conditions

When the system parameters are located at the triple point (ν_t, ε_t) and zero-flux boundary conditions are considered, the trivial state $(u = v = 1)$, which corresponds to the most stable mode, dominates the Turing and Hopf modes and is the only one that persists for any initial condition.

When the parameter ε is varied slightly along the line separating the Hopf and the Turing regions ($\nu = -1.0; 0 < \varepsilon - \varepsilon_t \ll 1$), different behaviors can be observed as a function of the initial conditions, namely; (a) central peak (CP) initial condition, which consists of a perturbation of Chua's circuits located in the central region (from circuit 225 to circuit 275), to a u value much bigger than the equilibrium state. The rest of the circuits are assumed to be operating at the equilibrium value ($u \cong 1$). (b) random (R) initial conditions, which consist of a perturbation of each circuit to a u value around the equilibrium position. In both cases, the v variable is assumed to be equal to its equilibrium value ($v \cong 1$).

For any ε value in the vicinity of the triple point $(2.0 < \varepsilon < 2.05)R$ initial conditions were unable to create Turing structures; however, it does give rise to the appearance of an oscillatory solution (Hopf mode). On the other hand, for CP initial conditions, different behaviors were observed for different ε values. Thus, for $\varepsilon \in (2.0, 2.001273)$ Hopf (i.e., oscillatory) solutions were obtained, and for (2.001274, 2.05) Turing (i.e., stationary) solutions were obtained. In Fig. 2(a) and (b), these behaviors are shown for slightly different values of ε.

In spite of the fact that both solutions proved to be stable against small perturbations once the final state had been reached, for those values of (ν, ε) near the Hopf–Turing transition, but in the Hopf region, an instantaneous small random perturbation (Δu) applied to each circuit during the transient state was sufficient to generate a Turing pattern, and not the Hopf solution that would be predicted for these parameter values.

Fig. 3(a) and (b) summarizes the dependence of the system behavior on the initial conditions. The amplitude of the solutions is represented as a function of the parameter ε. For oscillatory solutions, the amplitude represents the difference between the extremum values of each variable along the limit cycle. On the contrary, for Turing solutions, the amplitude represents the distance between the maximum and the minimum value of each variable in the stationary structure.

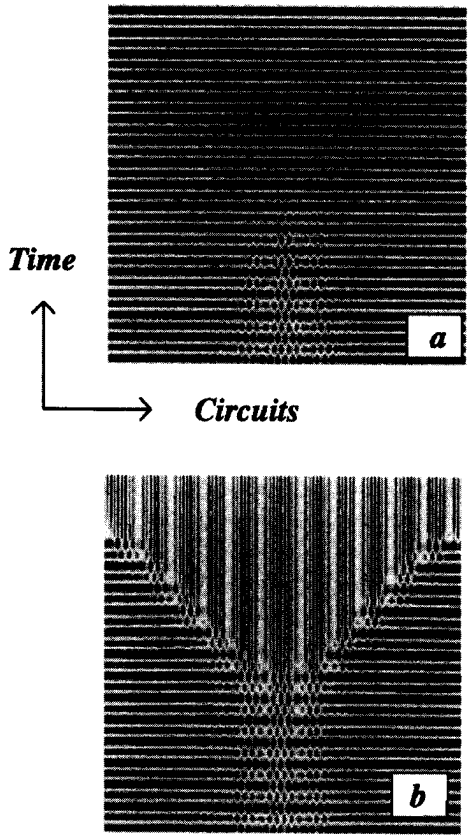

Fig. 2. Hopf and Turing evolution. For the same set of parameters related in Fig. 1 and $\nu = -1$, two qualitatively different system evolutions were observed for the same initial (CP) and boundary (zero-flux) conditions, and slightly different values of ε. In (a), for $\varepsilon = 2.001273$, a Hopf solution was obtained and in (b), for $\varepsilon = 2.001274$, a Turing solution was obtained. Observe that in the top of (a), parallel horizontal lines of smoothly varying gray scale levels repeat *periodically* in time, independently of the spatial (horizontal) position. This means all circuits are synchronized and oscillate with a common waveform. In (b), however, near the top when transients have disappeared, we obtain *constant vertical* lines (independent of time) whose gray-scale value varies smoothly along the spatial direction in a *periodic* manner, which by definition constitutes a Turing pattern.

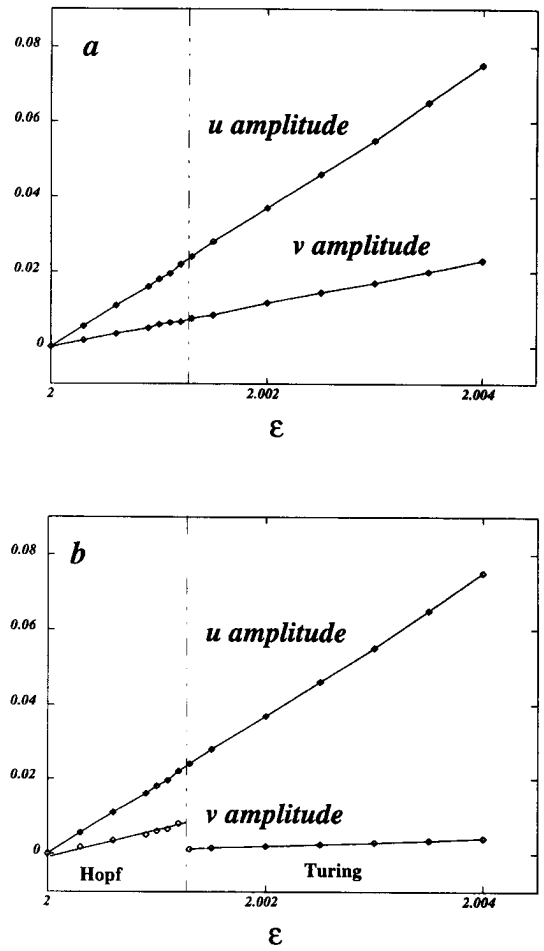

Fig. 3. Amplitude of (u, v) in Turing and Hopf solutions. The amplitude of both variables, calculated as explained in the text, are plotted as a function of ε for different (CP) and (R) initial conditions and zero-flux boundary conditions. In (a), for R initial conditions, the final state is always a Hopf solution whose amplitude (u and v variable) increases linearly with ε. In (b), for CP initial conditions, the behavior shifts from Hopf to Turing within the ε interval (2.001273, 2.001274). The u amplitude is continuous (does not change abruptly) at the transition point while the v amplitude has a discontinuity at this point, though it increases linearly both before and after the transition. Note that the u amplitude is the same in both figures and the v amplitude is only equal in the interval $\varepsilon \in (2.0, 2.001273)$ where a Hopf solution is obtained for any initial condition. The set of parameters was the same as in Fig. 2.

B. Influence of Boundary Conditions

Let us now investigate the effects of the boundary conditions assuming a fixed initial condition. In this section, only R initial conditions will be considered. Note that, although one can analyze the shape of the structures when only spatial terms are considered by solving an homogeneous eigenvalue problem [4], such analysis does not provide any additional information on the system evolution when placed near a triple point.

We have observed that for $\nu = -1.0, 0 < \varepsilon - \varepsilon_t \ll 1$, and imposing the Dirichlet[2] boundary conditions $u(0) = v(N + 1) = 1.0$ and $v(0) = v(N + 1) = 1.0$, where $u = v = 1.0$ is the equilibrium position and N the number of circuits in the array, the system evolves into a Turing pattern whose peaks are different near the boundaries. The temporal evolution of an R initial condition converges to the Turing structures shown in Fig. 4 when the Dirichlet boundary condition previously related was imposed. At some instant after the structures have stabilized, the amplitudes of the peaks close to the boundaries are significantly larger.

[2]A boundary condition is usually called a Dirichlet condition if the value of each variable is fixed at each boundary. In this case, we solve the circuits in the array (form 1 to N) and we fixed the values of both variables (u, v) in the circuits 0 and $N + 1$. These values are used to calculate the spatial derivatives in circuits 1 and N.

C. Influence of Random Changes in ν and ε in the Proximity of a Triple Point

Until now, we have assumed all cells to have exactly the same dynamics; i.e., every circuit has the same parameters and diffusion properties. This does not represent a realistic case either in biological or chemical systems. Even from an electronic circuit point of view, each circuit has a tolerance bigger than 1%. Even though the variation of the parameters can have some influence on system behavior [13], [18], this effect is merely quantitative when the parameters are

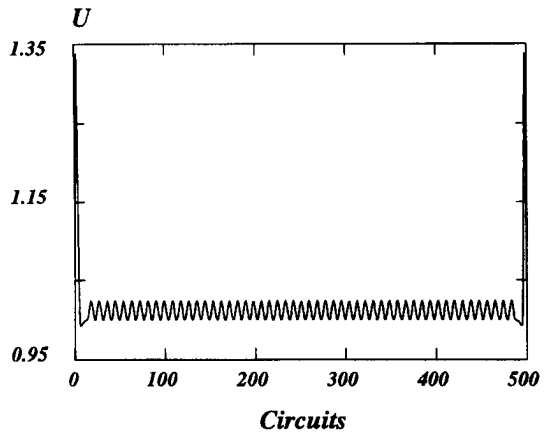

Fig. 4. Turing structure obtained with Dirichlet boundary conditions $(u(0) = v(0) = 1$ and $u(N+1) = v(N+1) = 1$, where $N = 500$ is the number of circuits in the array). For the set of parameters given in Fig. 2, $\varepsilon = 2.001273, R$ initial conditions Turing structures were obtained. Note that the amplitude of the peaks is much bigger near the boundaries.

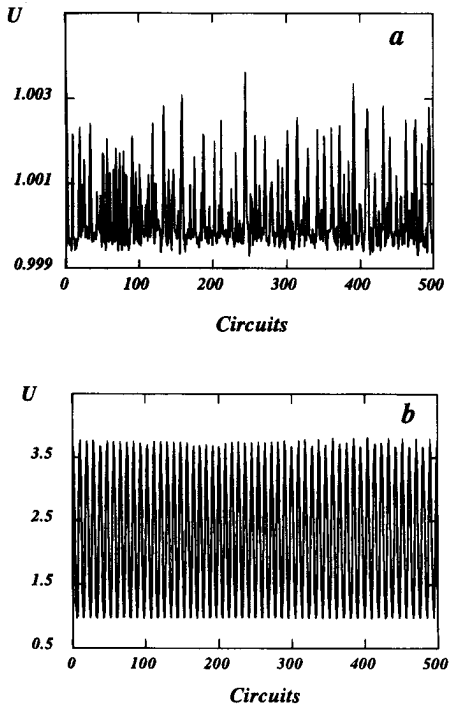

Fig. 5. Effect of $\Delta\varepsilon$ applied near or far from a triple point. Different Turing patterns were obtained when a small white noise was added to the ε parameter both in the vicinity of the triple point, and far from it. In (a) $(\varepsilon = 2, \nu = -1)$ a "*noisy*" stationary pattern was obtained, while in (b) $(\varepsilon = 2, \nu = -2)$ a Turing pattern (with a characteristic wavelength) was obtained. In both cases, we choose the same set of parameters as those in Fig. 1 and $\Delta\varepsilon = 10^{-3}$.

distributed around a point where there exists only one possible state; namely, excitable, Turing or Hopf. We now show that, if the values of (ν, ε) vary randomly around a triple-point, new patterns can be observed.

In the following numerical simulations, we have carried out all calculations with zero flux boundary conditions and CP initial conditions, since this allows us to obtain different behaviors when ε is varied along the line $\nu = -1$. In all

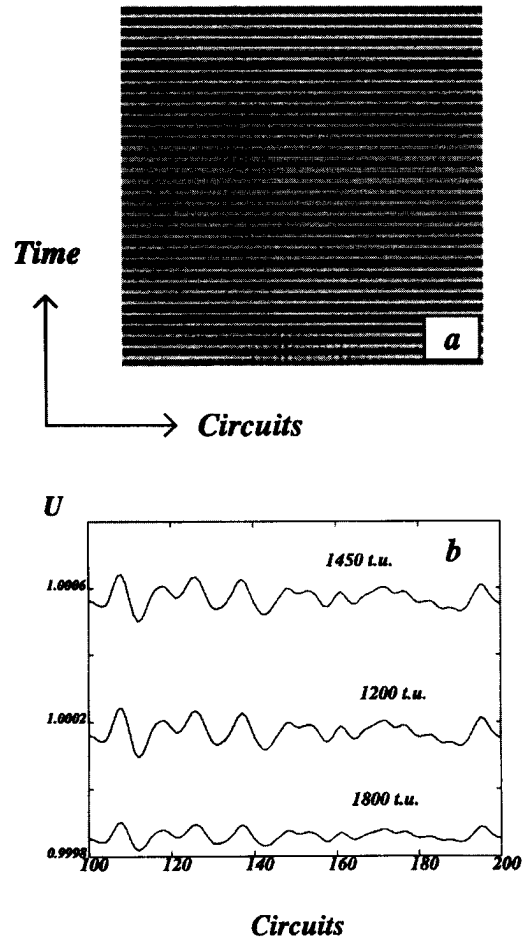

Fig. 6. A Turing mode superimposed on top of a Hopf mode. For the set of parameters given in Fig. 1 and $(\varepsilon = 2.001275, \nu = -1)$ the final state (a) is similar to the oscillatory (Hopf) solution in Fig. 2(a). However, in (b) observe that for different time instants, there is a relatively small stationary Turing structure superimposed on top of a large-amplitude oscillatory (Hopf) solution.

calculations, a random white noise was added to the parameter values in such a way that

$$\varepsilon \in [\varepsilon_o - \Delta\varepsilon/2, \varepsilon_o + \Delta\varepsilon/2]$$
$$\nu \in [\varepsilon_o - \Delta\nu/2, \nu_o + \Delta\nu/2] \quad (8)$$

where $\Delta\varepsilon$ and $\Delta\nu$ are the amplitudes of the noise in both variables.

Initially, a random distribution around (ν_t, ε_t) was considered, in all cases the system attained a stationary final state, similar to Turing structures but with peaks of different amplitudes and different wavelengths between peaks. We called them "*noisy Turing*" patterns since they look like a noisy spatial signal, but stationary in time. Note that, when Turing structures are considered, the final state corresponds to the most probable mode, the one with the biggest positive real part [4], [14]. However, near a triple point, several modes have a nearly identical real part and, thus, they spread with nearly identical velocity. Fig. 5 shows for the same noise amplitude $(\Delta\varepsilon)$, two different final states; the pattern in Fig. 5(a) is observed when is near the triple point, whereas that of Fig. 5(b) is obtained when is far from the triple point.

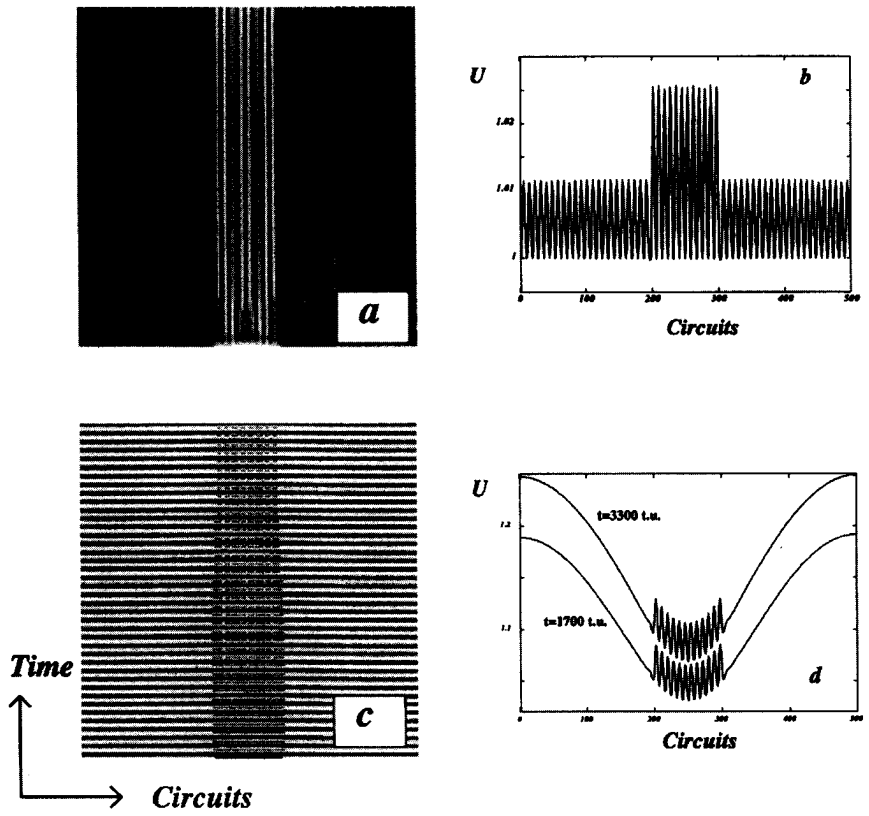

Fig. 7. Effect of inhomogeneities near the Hopf–Turing transition. For the set of parameters given in Fig. 1 and with circuits (200, 300) below the line of Hopf–Turing transition ($\nu = -1.005$), the rest of the circuits being above this line ($\nu = -0.995$), the system behavior was studied near and far from the triple point ($\varepsilon = 2.0$). For $\varepsilon = 2.01$ (near the triple point), one can observe (a) how the circuits in the Turing region induce a Turing behavior on those circuits located in the Hopf region. In the steady one can observe a Turing structure with two different amplitudes as shown in (b). For $\varepsilon = 2.2$ (far from the triple point), observe (c) how an oscillatory (Hopf) solution remains in the Hopf region and both modes (Hopf and Turing) remain coupled in the Turing region. In (d) this behavior can be observed for two different time instants. In this case, the amplitudes of both modes in the interval (200, 300) are approximately the same.

Another system behavior can be observed when the value is chosen close to the point where, for CP initial conditions, the final state changes from a Hopf to a Turing solution. We have considered $\nu = -1$ and $\varepsilon = 2.001275$, which corresponds to the appearance of Turing structures for CP initial conditions and zero-flux boundary conditions. Small random changes in $\varepsilon(\Delta\varepsilon < 2.5 \times 10^{-3})$ gave rise to Turing structures. During their formation a competition between several modes was observed but, eventually, only one remained. On the contrary, when $\Delta\varepsilon > 2.5 \times 10^{-3}, (\varepsilon_o - \Delta\varepsilon/2$ can become smaller than $\varepsilon_t)$ the noisy Turing patterns described above were observed.

On the other hand, when a small $\Delta\nu$ centered around ν_t and $\varepsilon = 2.001275$ were considered, different calculations with the same initial conditions (CP), parameter values, $\Delta\nu$ and zero-flux boundary conditions gave rise to different behaviors. In particular, a Turing or Hopf was obtained. The most unexpected behavior was observed in those cases when a Hopf solution was finally reached. In Fig. 6(a), observe that as time increases, the gray scale pattern becomes periodic (near the top edge) in time and nearly uniform in space. To show the pattern along the spatial direction (horizontal) is not homogeneous even after the transients had settled down, we have magnified the instantaneous value of $u(t)$ at three time instants; namely, $t = 1200$ t.u. (time unit), 1450 t.u. and 1800 t.u. Observe the relatively small spatial variations remain almost identical (local extreme points occur at the same position), independent of time, and constitutes therefore a small-amplitude Turing pattern, superimposed on top of a large amplitude Hopf oscillation.

D. Influence of Spatial Inhomogeneities

In this final section we study the system behavior in the proximity of a triple point when most of the circuits are located in the Hopf region near the transition line and a small group of circuits is located in the Turing region very close to the transition line.

Throughout our calculations, for circuits in the interval (200, 300) the parameter ν is chosen as $\nu = 1.005$ (Turing), and $\nu = 0.995$ (Hopf) for the remaining circuits, with zero-flux boundary conditions and R initial conditions. We have considered an interval consisting of 100 circuits in order to improve our image quality, but qualitatively similar results would be obtained for any interval containing more than ten circuits.

In Fig. 7(a) one can observe the system evolution when ε is chosen close to the triple point ($\varepsilon = 2.01$). The circuits in the Turing region (between 200 and 300) are able to

induce the appearance of Turing structures in the Hopf region, giving rise to a final state where two Turing structures of different amplitudes coexist. This coexistence can be observed in Fig. 7(b), which corresponds to a time instant after the structure had stabilized.

A different situation is shown in Fig. 7(c), which corresponds to a value far from the critical point ($\varepsilon = 2.2$). In this case, the oscillatory solution remains in the Hopf region while in the Turing region, the Turing mode is superimposed on top of the Hopf mode. In this case the amplitudes of both modes are similar, as shown in Fig. 7(d), where two different time instants are plotted.

REFERENCES

[1] A. M. Turing, "The chemical basis of morphogenesis," *Phil. Trans. R. Soc. London,* vol. B327, pp. 37–72, 1952.

[2] V. Castets, E. Dulos, J. Boissonade, and P. De Kepper, "Experimental evidence of a sustained Turing-type nonequilibrium chemical pattern," *Phys. Rev. Lett.,* vol. 64, pp. 2953–2956, 1990.

[3] Q. Ouyang and H. L. Swinney, "Transition from a uniform state to hexagonal and striped Turing patterns," *Nature,* vol. 352, pp. 610–612, 1991.

[4] J. D. Murray, *Mathematical Biology.* New York: Springer-Verlag, 1989.

[5] K. Lee, W. D. McCormick, J. E. Pearson, and H. L. Swinney, "Experimental observation of self-replicant spots in a reaction-diffusion system," *Nature,* vol. 369, pp. 215–218, 1994.

[6] T. Li and K. C. Nicolau, "Chemical self-replication of palindromic duplex DNA," *Nature,* vol. 369, pp. 218–221, 1994.

[7] W. N. Reynolds, "Dynamics of self-replicant patterns in reaction diffusion systems," *Phys. Rev. Lett.,* vol. 72, pp. 2797–2800, 1994.

[8] J. E. Marsden and M. McCracken, *The Hopf Bifurcation and Its Applications.* Berlin: Springer, 1976.

[9] P. De Kepper, J. J. Perraud, B. Rudovics, and E. Dulos, "Experimental study of stationary Turing patterns and their interaction with traveling waves in a chemical system," *Int. J. Bifurc. and Chaos,* vol. 4, no. 5, pp. 1215–1231, 1994.

[10] A. Rovinsky and M. Mezinguer, "Interaction of Turing and Hopf bifurcations in chemical systems," *Phys. Rev. A,* vol. 46, pp. 6315–6322, 1992.

[11] A. P. Muñuzuri, V. Pérez–Muñuzuri, V. Pérez–Villar, and L. O. Chua, "Spiral waves on a 2-D array of nonlinear circuits," *IEEE Trans. Circuits Syst.,* vol. 40, pp. 872–877, 1993.

[12] V. Pérez–Muñuzuri, V. Pérez–Villar, and L. O. Chua, "Propagation failure in linear arrays of Chua's circuits," *Int. J. Bifurc. and Chaos,* vol. 2, no. 2, pp. 403–406, 1992.

[13] V. Pérez–Villar, A. P. Muñuzuri, V. Pérez–Muñuzuri, and L. O. Chua, "Chaotic syncronization of a one-dimensional array of nonlinear active systems," *Int. J. Bifurc. and Chaos,* vol. 3, no. 4, pp. 1067–1074, 1993.

[14] V. Pérez–Muñuzuri, M. Gómez–Gesteira, A. P. Muñuzuri, L. O. Chua, and V. Pérez–Villar, "Sidewall forcing of hexagonal Turing patterns: Rombic patterns," *Physica D,* vol. 82, pp. 195–204, 1995.

[15] A. P. Muñuzuri, V. Pérez–Villar, M. Gómez–Gesteira, L. O. Chua, and V. Pérez–Villar, "Spatiotemporal structures in discretely-coupled arrays of nonlinear circuits: A review," *Int. J. Bifurc. and Chaos,* vol. 5, no. 1, pp. 17–50, 1995.

[16] L. O. Chua, "Dynamic nonlinear networks: State-of-the-art," *IEEE Trans. Circuits Syst.,* vol. CAS-27, no. 11, pp. 1059–1087, 1980.

[17] R. Madan, *Chua's Circuit: A Paradigm for Chaos.* Singapore: World Scientific, 1993.

[18] V. Pérez–Muñuzuri, M. Gómez–Gesteira, V. Pérez–Villar, and L.O. Chua, "Travelling wave propagation in a one-dimensional fluctuating medium," *Int. J. Bifurc. and Chaos,* vol. 3, no. 1, pp. 211–215, 1993.

Moncho Gómez-Gesteira, for a photograph and biography, see this issue, p. 671.

Vicente Pérez-Muñuzuri, for a photograph and biography, see this issue, p. 671.

Leon O. Chua (S'60–M'62–SM'70–F'74), for a photograph and biography, see this issue, p. 558.

Vicente Pérez-Villar, for a photograph and biography, see this issue, p. 671.